Current Cardiology Reports
https://doi.org/10.1007/s11886-024-02114-6

NUCLEAR CARDIOLOGY (V DILSIZIAN, SECTION EDITOR)

Recent Advances in Positron Emission Tomography Radiotracers to Image Cardiac Amyloidosis

Ardel J. Romero Pabón[1,2,3] · Olivier F. Clerc[1,2] · Shilpa Vijayakumar[1,2,3] · Sarah A. M. Cuddy[1,2,3] · Sharmila Dorbala[1,2,3]

Accepted: 2 August 2024

Abstract

Cardiac amyloidosis includes a group of protein-misfolding diseases characterized by fibril accumulation within the extracellular space of the myocardium and cardiac dysfunction. Cardiac amyloidosis has high mortality. Emerging radionuclide techniques have helped us to better understand disease pathogenesis, prognostication, and treatment response in cardiac amyloidosis.

Purpose of Review To review recent advances in molecular imaging of cardiac amyloidosis using amyloid PET radiotracers.

Recent Findings Multiple single center studies have shown that amyloid PET radiotracers allow definitive diagnosis and quantification of cardiac amyloid burden. These amyloid targeting tracers may provide means to improve early disease detection, risk stratification and treatment monitoring.

Summary Amyloid PET imaging may inform definitive imaging-based diagnosis for therapeutic decisions, risk stratification, and treatment monitoring. More research in unselected cohorts of patients with suspected cardiac amyloidosis is needed to optimize the clinical implementation of amyloid PET imaging.

Keywords Cardiac Amyloidosis · Positron Emission Tomography · Radiotracers

Introduction

Systemic amyloidosis is a group of protein-misfolding diseases where misfolded proteins accumulate as amyloid fibrils in the extracellular space [1–3]. Infiltration of the organs with amyloid fibrils leads to organ dysfunction. Cardiac amyloidosis (CA) occurs when these fibrils accumulate within the myocardial extracellular space causing extracellular space expansion, increased thickness of the myocardium, cardiomyocyte stretch, and in some cases cardiomyocyte injury and apoptosis [4]. Cardiac involvement causes significant morbidity from heart failure, cardiac arrhythmias, and conduction disturbances; but more importantly, it drives mortality in patients with systemic amyloidosis [2, 3, 5, 6]. CA is also an underrecognized cause of heart failure, especially in elderly patients with heart failure with preserved ejection fraction [2, 3]. Although there are multiple types of systemic amyloidosis, the two most common types that affect the heart are transthyretin amyloidosis (ATTR) and light-chain amyloidosis (AL). ATTR is caused by the misfolding of transthyretin and is the more prevalent disease type. Transthyretin is a tetrameric transport protein produced in the liver and is involved in the transport of thyroxine and retinol [7, 8]. ATTR amyloidosis can be further subdivided depending on its origin. Patients with amyloidogenic genes are categorized within the hereditary subtype, also called *'variant'* ATTR (ATTRv) [1]. In turn, those with genetically normal forms of the disease are classified as '*wild-type'* ATTR (ATTRwt) [1], previously referred to as senile or age-related ATTR. ATTR amyloidosis primarily affects the heart (ATTRwt), but it can also affect the musculoskeletal and nervous systems (which is more common in ATTRv), leading to clinical manifestations such as carpal tunnel syndrome, lumbar spinal stenosis, and biceps tendon rupture

✉ Sharmila Dorbala
sdorbala@bwh.harvard.edu

1 Division of Cardiology, Department of Medicine, Cardiac Amyloidosis Program, Brigham and Women's Hospital, Boston, Massachusetts, USA

2 Division of Nuclear Medicine and Molecular Imaging, Department of Radiology, Brigham and Women's Hospital, Boston, Massachusetts, USA

3 Cardiovascular Imaging Program, Division of Cardiology, Department of Radiology, Brigham and Women's Hospital, Boston, Massachusetts, USA

Published online: 13 August 2024

[9, 10]. Conversely, AL amyloidosis is a systemic plasma cell dyscrasia caused by the misfolding and deposition of immunoglobulin-derived light chains into multiple organs, such as the heart, kidneys, digestive system, liver, peripheral nerves, lungs, skin, etc. Amyloid fibrils from any type of precursor protein have a similar structure and are composed of protofilaments (protein layers with a generic cross β structure) and additional molecules such as glycosaminoglycans and serum amyloid P-component [2, 3, 11].

The pathognomonic histopathological feature of CA is fibril deposition demonstrating positivity on Congo Red staining and apple-green birefringence under polarized light [1, 12]. Once a histological diagnosis of amyloid is confirmed by staining, samples undergo mass spectroscopy or immunohistochemistry for further amyloid typing into AL, ATTR, or rarer forms of amyloidosis [13, 14]. While endomyocardial biopsy was the reference standard for diagnosis, contemporary diagnostic approaches allow the use of non-invasive imaging as a substitute for invasive biopsy in the right clinical context; particularly, for the diagnosis of ATTR-CA once plasma cell dyscrasias are excluded. Additionally, for patients with extracardiac biopsy-proven systemic AL amyloidosis and typical cardiac imaging features –or cardiac biomarkers release– endomyocardial biopsy proof is not needed to diagnose AL-CA [9, 10]. Once the diagnosis of amyloidosis is suspected, based on clinical and echocardiographic findings, cardiac magnetic resonance imaging (MRI) and radionuclide imaging have become the standard confirmatory methods to diagnose cardiac amyloidosis [9, 10]. It is worth noting that the combination of emerging therapeutic options and multi-modality imaging has shifted the disease paradigm from a delayed, under-recognized, and highly mortal condition to a more treatable condition when early diagnosis, treatment, and appropriate disease monitoring are instituted.

Standard echocardiography and cardiac MRI are powerful diagnostic tools as they provide measures to assess the structural and functional consequences of CA. However, these modalities do not directly image amyloid burden. In addition, native T1 mapping and extracellular volume (ECV) quantification by cardiac MRI are frequently used for tissue characterization in CA [15]. ECV quantification provides an estimate of disease burden, however, it is unable to accurately differentiate between amyloid fibrils deposition, inflammation, edema, and fibrosis. Furthermore, early stages of cardiac involvement are difficult to identify with echocardiography and cardiac MRI given the significant overlap in findings in other forms of cardiomyopathy [9, 10, 16].

In comparison, radionuclide techniques like Single-Photon Emission Computed Tomography (SPECT) imaging and Positron Emission Tomography (PET) imaging are based on amyloid-binding radiotracers offering several advantages [5, 9, 10]. Bone-avid tracer SPECT has become standard of care for the non-invasive clinical diagnosis of ATTR-CA in specific scenarios [17]. SPECT based ^{99m}Tc-bone avid tracer imaging for amyloidosis has been shown to have a high diagnostic yield for ATTR-CA. Moreover, SPECT bone-avid tracers are more specific than echocardiography and cardiac MRI for detection of CA. In addition, novel SPECT/CT techniques allow for absolute quantification of amyloid burden [18] which can be potentially helpful for early disease detection and for assessment of response to therapy. However, bone-avid tracer cardiac SPECT has certain limitations. Firstly, current SPECT interpretation is based on direct visual assessment by comparing myocardial uptake to bone uptake. Secondly, the binding mechanism of bone-avid radiotracers is not yet fully understood, and several clinical scenarios can lead to false positive test results (e.g., acute or subacute myocardial infarction). Bone-avid tracer SPECT can also be falsely negative in certain forms of ATTRv. Moreover, these tracers do not reliably image AL-CA or CA from other rare forms of amyloidosis [5, 17].

Many of these limitations can be overcome by current amyloid-binding PET radiotracers [11, 19]. A number of prior review articles have addressed SPECT imaging in ATTR-CA [20, 21] and readers are referred to those publications for more details on SPECT imaging of ATTR-CA. In this review, we will discuss recent advances in molecular imaging of CA using amyloid PET radiotracers and their increasing role in early disease detection, quantification of amyloid burden, prognostication, and future applications for disease monitoring.

Positron Emission Tomography (PET)

PET offers high temporal and spatial resolution and accurate attenuation correction that allows for accurate quantification of absolute myocardial tracer uptake [22]. Additionally, beta-amyloid tracer PET imaging has also been shown to have good diagnostic sensitivity and specificity for CA, especially for AL amyloidosis [11, 23, 24]. For these reasons, PET could become more relevant in clinical practice. However, to date, PET imaging is not universally used but emerging data supports its expanded use in the near future.

Multiple studies have shown that amyloid-binding PET radiotracers [^{124}I-evuzamitide, as well as beta-amyloid tracers (^{11}C-Pittsburgh compound-B, ^{18}F-florbetapir, ^{18}F-florbetaben, ^{18}F-flutemetamol)] allow earlier visualization of patterns of amyloid fibril deposition and quantification of cardiac and whole-body amyloid burden (Table 1). The beta-amyloid tracers were initially engineered to image cerebral amyloid deposits in Alzheimer's disease and are thioflavin T analogs [25]. They directly bind to the β-pleated motifs of amyloid fibrils, independently of its precursor protein, whereas the more novel ^{124}I-evuzamitide (^{124}I-p5 + 14) binds

Table 1 Summary of the PET radiotracers used for cardiac amyloidosis imaging

Tracer	Mechanism	Advantages	Disadvantages
^{11}C-PiB	Binds to β-pleated motifs	Larger body of evidence Role in disease risk stratification and fibril characterization Short half-life (20 min)	Requires onsite cyclotron Lower perforce in ATTR-CA Short scan time (30 min)
^{18}F-florbetapir ^{18}F-florbetaben	Binds to β-pleated motifs	Commercially available for brain imaging Does not require onsite cyclotron Identifies subclinical disease	Cannot reliably assess hepatic and renal amyloid deposition Lower perforce in ATTR-CA Short scan time (30 min) Longer half-life (110 min)
^{18}F-flutemetamol			Limited body of evidence with contradictory clinical utility Short scan time (30 min)
^{124}I-evuzamitide	Binds to glycosaminoglycans present in amyloid fibrils	Convenient unit dose radiotracer access May have better performance than other tracers in ATTR-CA Allows hepatic amyloid assessment	Long half-life (4.2 days) Higher effective radiation dose Long scan time (4–5 h between injection and scan acquisition) Greater positron range than fluorine which can lead to image degradation

to the abundant –and electronegatively charged– glycosaminoglycans present in amyloid fibrils [11, 26, 27]. Finally, ^{18}F-Na fluoride has been proposed to bind to ATTR fibrils through a poorly understood calcium-mediated mechanism (Fig. 1). Nonetheless, current evidence shows that ^{18}F-Na fluoride has poor myocardial uptake in CA (target to background ratio's often < 1.0 in CA) [28–31], which limits visual interpretation despite its colocalization to regions of late gadolinium enhancement in CMR [31]. Hence, we will not discuss this tracer in this review.

^{11}C-Labeled Pittsburg Compound-B (^{11}C-PiB)

^{11}C-PiB is one of the most studied and widely used amyloid agents for CA imaging. This tracer was first used to directly visualize myocardial amyloid deposition by Antoni et al. [32]. This group compared myocardial tracer uptake among 10 patients with AL and ATTR amyloidosis and 5 age-matched healthy volunteers to determine the impact of global and regional perfusion on ^{11}C-PiB retention [32]. They found myocardial tracer uptake to be visually evident in all the cases of CA while being absent among the healthy subjects. Lee et al. [33] confirmed these findings in their prospective multimodality cohort study of 22 patients with AL amyloidosis (including 15 patients with biopsy-proven CA) and 10 healthy volunteers. They found ^{11}C-PiB PET to have a comparable sensitivity and specificity to LGE on cardiac MRI. More importantly, they reported lower standardized uptake values (SUV) in patients with biopsy-proven CA who underwent previous chemotherapy in comparison to treatment-naïve patients. These findings signaled the potential role of this technique for disease burden and therapy response monitoring, as ^{11}C-PiB uptake could potentially be used as a surrogate of new myocardial light chain deposition.

Another study [34] compared myocardial tracer uptake of ^{11}C-PiB in 10 patients with biopsy-proven ATTRv amyloidosis and 5 healthy controls and found elevated myocardial uptake in all the amyloid cases but not in the control group. In this study, Pilebro et al. [34], also showed that ^{11}C-PiB can give us insight into the disease pathogenesis due to its preferential and heterogenous binding to type B fibrils (full-length only fibrils often seen in early-onset disease), in comparison to its lower and homogeneous biding to type A fibrils (fragmented and full-length fibrils often seen in late-onset disease). By contrast, Takasone et al. [35] studied 17 patients with AL amyloidosis, 22 with ATTRv and 8 with ATTRwt and reported a positive ^{99m}Tc-pyrophosphate (PYP) uptake and negative ^{11}C-PiB uptake pattern (PYP pattern) observed in patients with late-onset V30M ATTRv, non-V30M ATTRv, and ATTRwt amyloidosis. Complementarily, they observed a positive ^{11}C-PiB uptake and negative ^{99m}Tc-PYP uptake pattern (PiB pattern) in patients with AL amyloidosis and early-onset V30M ATTRv. These findings suggest lower sensitivity of ^{11}C-PiB for certain forms of ATTR-CM and highlight the potential complementary role of different imaging methods along with genetic testing.

Subsequently, a larger dual-center study done by Rosengren et al. [36] confirmed the excellent sensitivity and specificity of ^{11}C-PiB by studying 36 patients with multiple forms of CA (15 AL, 16 ATTRwt, and 7 ATTRv) and comparing their tracer uptake to a control cohort composed by 8 healthy volunteers and 7 patients with non-amyloid-hypertrophic cardiomyopathy [36]. Two particularly important findings of this study were: 1) the high prevalence of ^{11}C-PiB uptake among CA patients without increased cardiac wall thickness

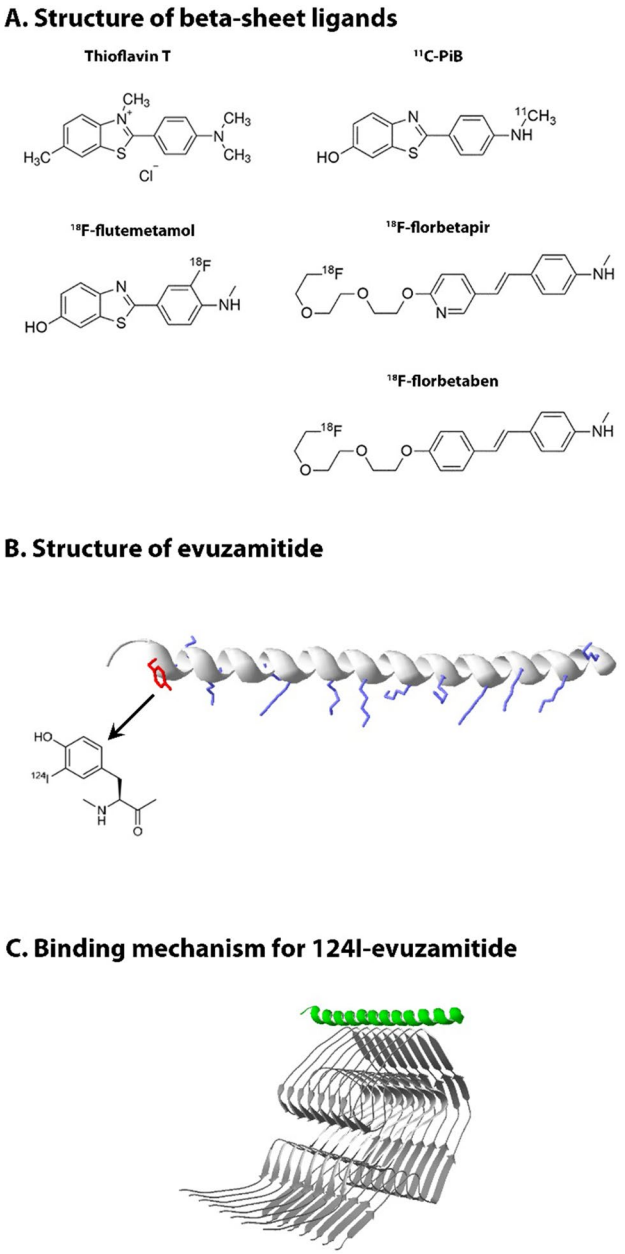

Fig. 1 **A** Molecular structures of various amyloid radiotracers. **B** and **C** the synthetic polypeptide ^{124}I-evuzamitide binds to the negatively charged glycosaminoglycans present in amyloid fibrils. Figure **A** was adapted from Uzuegbunam et al. [59] [Creative Commons CC BY 4.0 license]. Figures **B** and **C** were provided courtesy of Dr. Jonathan Wall, University of Tennessee)

(reinforcing that ^{11}C-PiB PET may be able to detect early disease stages), and 2) the relatively higher uptake values for ^{11}C-PiB found in patients with AL amyloidosis (highlighting the role of this marker in AL disease characterization).

More recently, Choi et al. [37] proved in 58 patients, that ^{11}C-PiB uptake, visually interpreted as positive or negative, is also an independent predictor of mortality in patients with AL cardiac amyloidosis, even after individually adjusting for conventionally used clinical disease biomarkers during their small subgroup analyses (troponin I, NT-pro-BNP, and absolute difference between involved and uninvolved free light chains, dFLC) [37]. These findings provide pilot data on risk stratification with ^{11}C-PiB PET in AL amyloidosis. However, more evidence is needed on whether PET imaging should be included during risk stratification in patients with AL amyloidosis.

^{18}F-Florbetapir

Florbetapir is a stilbene derivate which makes it structurally different from ^{11}C-PiB. Additionally, this tracer is labeled with ^{18}fluorine (^{18}F) which has a 2-h half-life and can be transported as unit doses from a commercial cyclotron [11]. Importantly, ^{18}F-florbetapir binds to both AL and ATTR fibrils but has been noted to have a higher affinity for AL fibrils during in vitro studies [38]. In 2014, Dorbala et al. [39] presented the first pilot study using this agent for cardiac amyloidosis imaging. In this study, the authors compared the performance of ^{18}F-florbetapir PET in 9 subjects with documented CA (from which 7 had positive myocardial biopsies and 2 had positive extracardiac biopsies and typical imaging features) and 5 healthy controls. They found diffuse biventricular ^{18}F-florbetapir uptake among all amyloid subjects but not in the control group. They reported overall higher uptake values in patients with AL amyloidosis despite their lower myocardial thickness when compared to those with ATTR amyloidosis. Low myocardial uptake was also noted in AL treated subjects, suggesting that myocardial florbetapir uptake may reflect disease activity as well as amyloid burden.

Ehman et al. [40] studied whole-body ^{18}F-florbetapir PET to assess its performance in systemic AL amyloidosis in a cohort of 40 patients with biopsy-proven AL (30 with active disease, and 10 in hematologic remission). They found that –both quantitative and visually graded– ^{18}F-florbetapir uptake detected more organ involvement than did the international consensus criteria for organ involvement and clinical manifestations [41]. ^{18}F-florbetapir identified amyloid deposition in the organs of patients who were thought to be in hematologic remission. Similar findings were reported by other investigators using various other amyloid PET radiotracers [42–45].

Additionally, ^{18}F-florbetapir PET imaging may be useful to identify pulmonary involvement noninvasively [46]. Pulmonary amyloid deposits are very common in patients with AL-CA [47]. In a study done by Khor et al. [46], they compared ^{18}F-florbetapir uptake between 58 patients with biopsy-proven AL amyloidosis and 9 control subjects (5 without amyloidosis and 4 with ATTR-CA). They found

intense and homogenous pulmonary tracer uptake in 12% of the AL patients, most likely representing diffuse alveolar-septal amyloidosis (Fig. 2). Remarkably, the group of patients without visually apparent pulmonary ^{18}F-florbetapir uptake also had threefold higher lung uptake when compared with controls. Notably, the intense ^{18}F-florbetapir pulmonary distribution volume (derived from kinetic modeling analyses) was increased and was not related to lung perfusion assessed by ^{11}C-acetate lung uptake, supporting that this finding represents AL amyloidosis rather than heart failure-related lung tracer uptake [46].

Moreover, ^{18}F-florbetapir PET imaging provides insights into the preclinical disease process. In a study performed by Cuddy et al. [48], the authors compared ^{18}F-florbetapir retention indexes among 3 predefined groups of patients: 25 patients with active AL amyloidosis with cardiac involvement (active-CA), 10 with active AL amyloidosis but without cardiac involvement by conventional criteria and normal serum cardiac biomarkers (active-non-CA) [41], and 10 patients with AL amyloidosis with cardiac involvement but in remission for at least 1 year (remission-CA). They found that ^{18}F-florbetapir uptake was present in all the subjects, irrespectively of other test results, but was distinctly elevated in patients with cardiac involvement regardless of their disease status (active-CA and remission-CA vs active-non-CA). By comparing the retention indexes of ^{18}F-florbetapir and other cardiac MRI and echocardiographic findings among these groups, they showed that ^{18}F-florbetapir uptake may be positive even in patients with normal cardiac MRI and echocardiogram findings, showcasing the ability of PET imaging to detect subclinical disease and confirming that amyloid fibrils deposition is the cause of early ECV changes in cardiac MRI (Fig. 3) [48]. As mentioned previously, precise identification of organ involvement in systemic AL amyloidosis is vital given its prognostic and therapeutic implications. Therefore, the high diagnostic sensitivity provided by ^{18}F-flobetapir PET imaging has the potential to inform treatment (e.g., to determine if a patient is a candidate for stem cell transplantation) and allow non-invasive monitoring of the disease (Fig. 4) [11].

More recently, Datar et al. [49] proved that ^{18}F-florbetapir PET identifies preclinical right ventricular involvement in AL amyloidosis. In their prospective cohort study of 106 participants with systemic AL amyloidosis, they found that ^{18}F-florbetapir PET was able to detect amyloid deposition in 40% of the participants who did not meet conventional

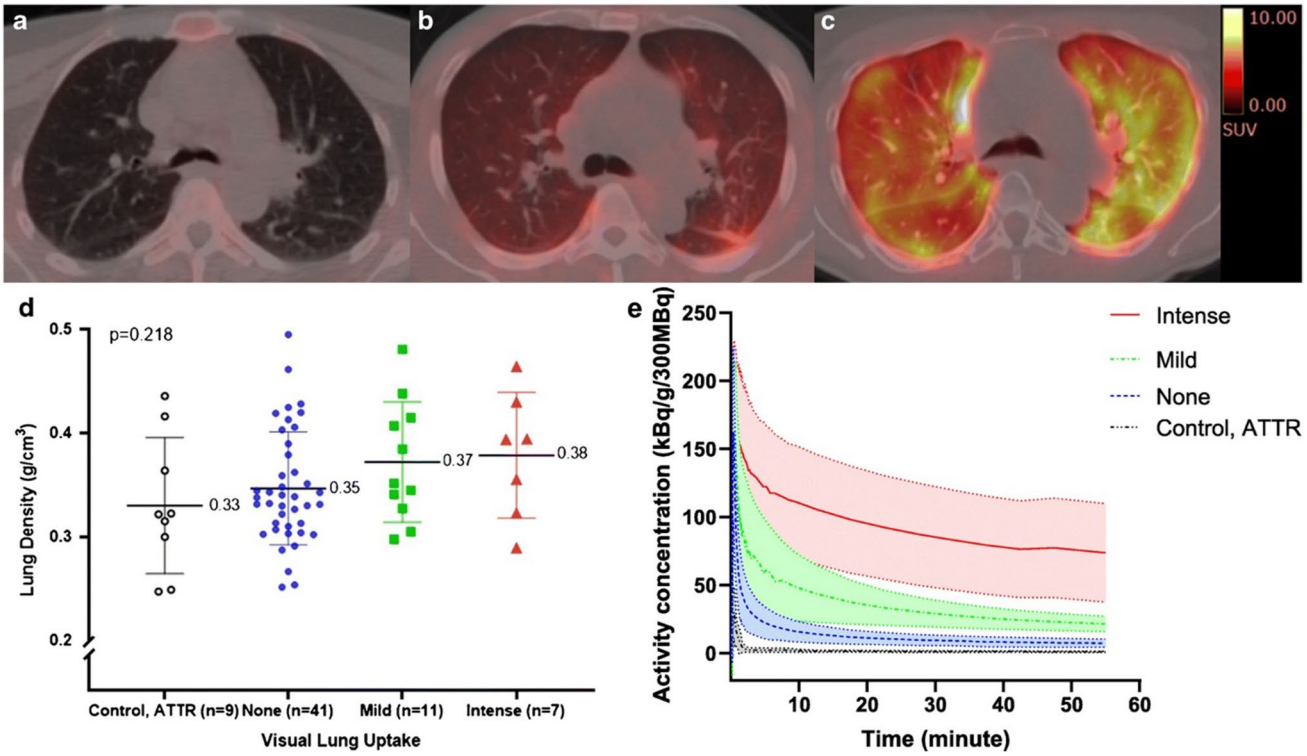

Fig. 2 ^{18}F-florbetapir pulmonary tracer uptake. ^{18}F-florbetapir PET/CT images of three patients with **a** no significant tracer uptake, **b** diffuse mild uptake, and **c** diffuse intense uptake, respectively. Of note, CT average lung densities did not differ among patients with different degrees of tracer uptake, and the control group (**bottom row**, **d**). Additionally, the rate of tracer washout was slowest in subjects with intense uptake and fastest among controls (**bottom row**, **e**). (Reprinted with permission from Khor et al. [46]; permission conveyed through Copyright Clearance Center, Inc.)

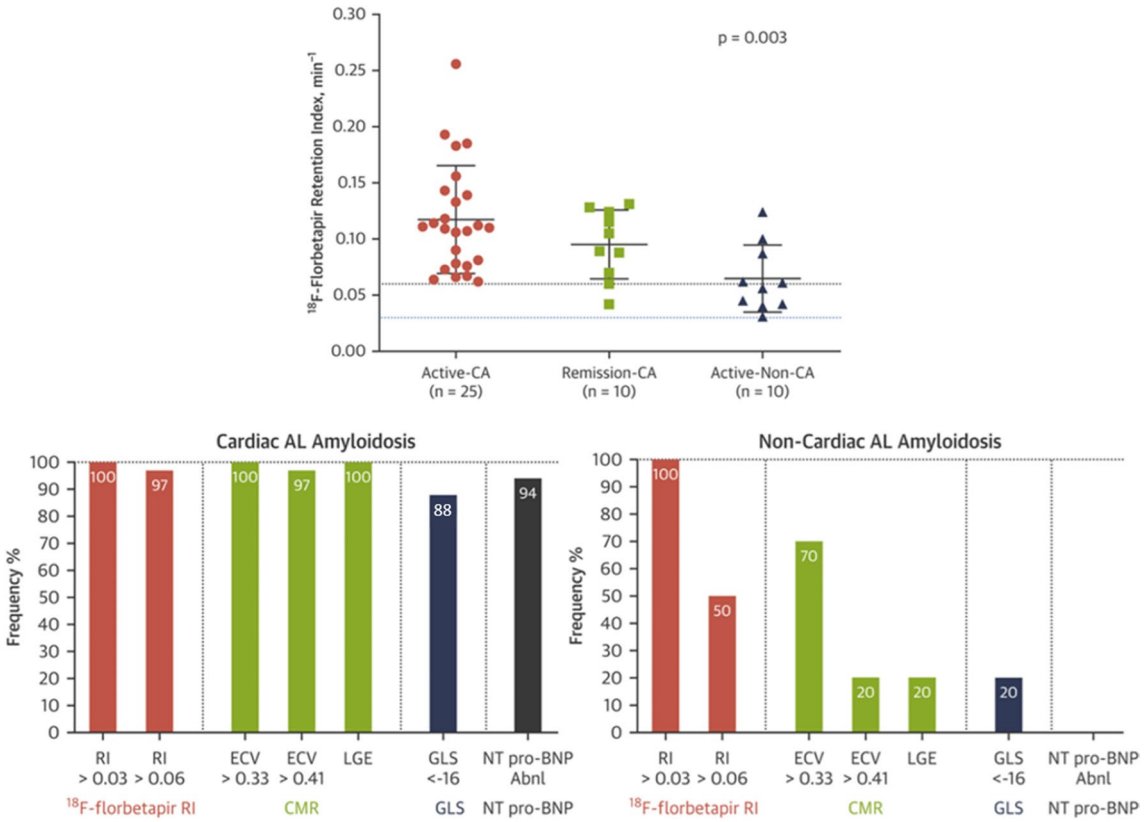

Fig. 3 Imaging findings in different groups of patients with AL amyloidosis. The **top row** shows the distribution of cardiac MRI ECV values in patients systemic AL amyloidosis with cardiac involvement (active-CA), without cardiac involvement by conventional criteria (active-non-CA), and patients with cardiac involvement in remission for at least 1 year (remission-CA). The *dotted blue line* represents the cutoff value to diagnose the presence or absence of CA while the *dotted black line* represents the upper threshold of normal observed in healthy controls. The p-value listed in the figure is the cross-group comparison. The **bottom row** shows the prevalence of abnormal indexes of cardiac amyloid deposition in these groups. Cardiac AL Amyloidosis = active-CA and remission-CA. Non-Cardiac AL Amyloidosis = active-non-CA. (Reprinted with permission from Cuddy et al. [48], with permission from Elsevier.)

criteria for cardiac involvement [41]. Of note, left ventricular (LV), right ventricular (RV) and pulmonary amyloidosis could lead to pulmonary hypertension in AL amyloidosis [50]. However, this study showed that RV amyloid, but not LV amyloid or lung amyloid, is a key driver of RV dysfunction. They also noted that quantitatively measured RV amyloid was able to independently predict major adverse cardiovascular events [49]. These findings highlight the central role of direct right ventricular amyloid deposition in the pathogenesis of AL amyloid-induced right ventricular dysfunction.

Finally, in a recent study done by Clerc et al. [51], the authors prospectively followed 81 patients with newly diagnosed systemic AL. They found that LV amyloid burden (quantified as the percentage of injected dose of ^{18}F-florbetapir, %ID) is a significant predictor of major adverse cardiovascular events (MACE) and all-cause death (Fig. 5). They also provided insights into the mechanistic process linking amyloid burden and MACE by conducting novel mediation analyses. They found that the association between ^{18}F-florbetapir LV %ID and MACE was primarily mediated by an indirect pathway involving NT-pro-BNP elevation [51], cardiomyocyte stretching and heart failure. This analysis explained why the adjustment by Mayo AL stage distorts the association between ^{18}F-florbetapir LV %ID and outcomes. This is one of the first studies to report the association between molecular cardiac amyloid burden, Mayo AL staging, and clinical outcomes.

Other Radiolabeled Thioflavin-T Derivates

Other radiolabeled PET tracers include ^{18}F-florbetaben and ^{18}F-flutemetamol. They both have shown promising results for the detection of both ATTR and AL amyloidosis. ^{18}F-florbetaben was first studied by Law et al. [52] among 10 patients with ATTR and AL amyloidosis and 4 controls with hypertensive heart disease. By using a LV myocardial ^{18}F-florbetaben mean standardized uptake values or a retention index cutoff of 40%, they found ^{18}F-florbetaben to

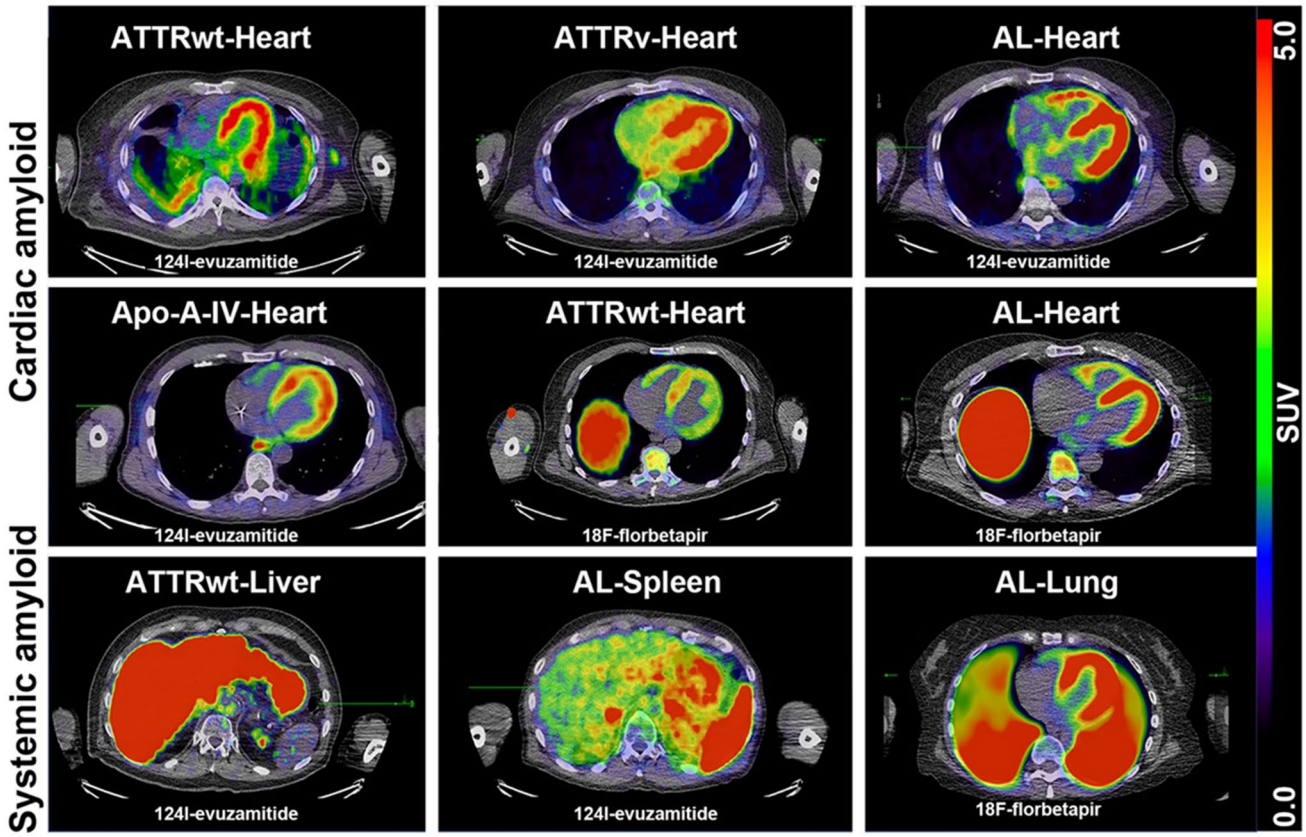

Fig. 4 Myocardial (**top 2 rows**) and systemic organ (**bottom row**) uptake of ^{18}F-florbetapir and ^{124}I-evuzamitide in patients with various forms of amyloidosis. Liver uptake is physiologic with ^{18}F-florbetapir imaging. Amyloid PET tracers bind to various types of amyloid fibrils and can image amyloid deposition in the cardiac and extracardiac tissues. Apo-A-IV = Apolipoprotein AIV. (Reprinted with permission from Dorbala et al. [11].)

be able to differentiate between amyloid and hypertensive cases. Tracer retention was also correlated with both global left ventricular longitudinal and right ventricular free wall longitudinal strains via inverse curve relationship. Another study [53] of 22 patients with clinically proven or suspected CA revealed different ^{18}F-florbetaben between amyloid subtypes (with AL being higher). More importantly, they also found changes in tracer retention among 4 patients who received follow-up ^{18}F-florbetaben PET after treatment initiation, these changes were correlated with treatment response. Notably, the first study that evaluated the role of ^{18}F-flutemetamol PET in cardiac amyloidosis demonstrated positive results in 8 out of 9 patients [54]. However, Papathanasiou et al. [55] recently studied the accuracy of ^{18}F-flumetamol in 12 patients with cardiac amyloidosis (10 with ATTR and 2 with AL) and 5 non-amyloid heart failure cases. In their study, only 2 patients with CA demonstrated increased tracer uptake raising questions about ^{18}F-flumetamol utility and reproducibility. More research is needed to further elucidate why these findings contradicted previously available reports, but it is worth mentioning that the tracer injection dose for this study was relatively low, and the post-injection images were collected at different times across studies. Additionally -because they only included 2 patients with AL amyloidosis- these study results are not applicable to AL amyloidosis.

^{124}I-Evuzamitide

^{124}I-evuzamitide (^{124}I-p5 + 14) is a synthetic polypeptide with positively charged lysine side chains that binds to the negatively charged glycosaminoglycans of amyloid fibrils [11, 26, 27].^{124}I-evuzamitide is a novel tracer, developed by Dr. Jonathan Wall [27, 56], that has been used for the imaging of cardiac amyloidosis and it is thought to have pan-amyloid binding properties. Unlike ^{18}F-based radiotracers, ^{124}I-evuzamitide can quantify hepatic and possibly renal amyloid (Fig. 4). Moreover, a therapeutic monoclonal antibody fusion protein with a similar amyloid-biding peptide is currently under investigation for amyloid fibril removal [57]. Clerc et al. [19] recently published the results of their pilot study of 26 patients with ATTRwt, AL, and ATTRv amyloidosis, and control participants comparing the performance

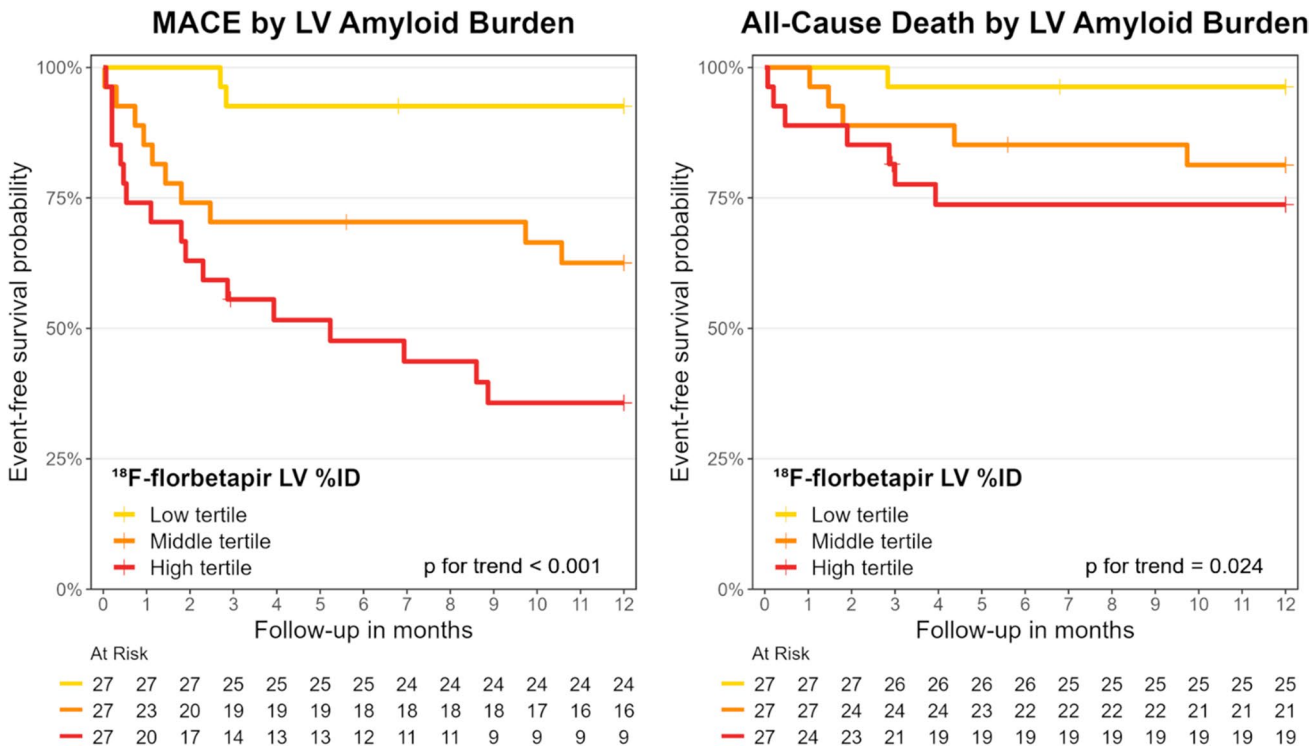

Fig. 5 Kaplan-Meier curves for MACE and all-cause death based on left ventricular amyloid burden. Left ventricular amyloid burden was assessed by tertiles of ^{18}F-florbetapir uptake quantified as percentage of the injected dose. The p-values in each graph correspond to the log-rank tests performed. LV = Left ventricular. %ID = percentage of the injected dose. MACE = Major Adverse Cardiovascular Events (all-cause mortality, heart failure hospitalization or cardiac transplantation). (Reprinted with permission from Clerc et al. [51], with permission from Elsevier.)

of ^{124}I-evuzamitide to ^{18}F-florbetapir. They found that ^{124}I-evuzamitide uptake was significantly higher in patients with both ATTRwt and AL amyloidosis when compared to control participants, accurately discriminating cases of amyloid cardiomyopathy from controls. Moreover, they found that ATTRwt burden quantification may be more accurate with ^{124}I-evuzamitide than with ^{18}F-florbetapir. [19].

Simultaneously, Wall et al. [58] demonstrated similar results while using ^{124}I-evuzamitide to image cardiac and systemic amyloid deposits in patients with various forms of systemic amyloidosis (23 with systemic AL amyloidosis, 2 with localized AL amyloidosis, 15 with ATTRv, 5 with ATTRwt, and 5 with other amyloid types).

Conclusions

Advances in multimodal imaging and the development of targeted therapies have transformed the management of systemic amyloidosis. Amyloid PET imaging offers several advantages when compared with other imaging techniques, not only given the unique properties of this modality, but also due to the molecular revolution surrounding the radiotracers that are being used in this modality. Amyloid PET imaging provides high diagnostic sensitivity and specificity, and has shown promising results for early disease detection, amyloid burden quantification, risk stratification of patients, and treatment response monitoring. The ability these tracers to accurately visualize amyloid fibrils deposition in the heart and other organs may inform therapeutic decisions and treatment monitoring in the near future. However, data on the efficacy of amyloid PET imaging is still limited and continued research is still needed to optimize its clinical implementation.

Author Contributions Drs. Romero Pabón AJ, Clerc OF, Vijayakumar S, Cuddy SAM, and Dorbala S contributed to the conception, design, and drafting of the manuscript. Drs. Romero Pabón AJ, Clerc OF, Cuddy SAM, and Dorbala S provided critical intellectual review. Drs Romero Pabón AJ, and Dorbala S prepared all the figures and tables. Author disclosures are explicitly stated within the manuscript, and all authors have read and approved the final version, meeting the guidelines for authorship.

Funding Romero Pabón: NIH funding: T32 HL 094301. Clerc: Research fellowship from the International Society of Amyloidosis and Pfizer. Vijayakumar: NIH funding: T32 HL 094301. Research funding from the Amyloidosis Foundation. Cuddy: NIH funding: K23 HL 166686-01. American Heart Association funding: 23CDA857664. Consulting fees from Ionis Pharmaceuticals, AstraZeneca, BridgeBio,

Novo Nordisk, and Alexion. Investigator-initiated research grant from Pfizer. Dorbala: NIH funding: K24 HL157648. Consulting fees: Pfizer, GE HealthCare, AstraZeneca, Novo Nordisk, WebMD, and MedTrace. Investigator-initiated grants from Pfizer, GE Healthcare, Attralus, Siemens, and Philips.

Data Availability No datasets were generated or analysed during the current study.

Compliance with Ethical Standards

Conflict of Interests The authors declare no competing interests.

Human and Animal Rights and Informed Consent This article does not contain any studies with human or animal subjects performed by any of the authors.

References

1. Buxbaum JN, Dispenzieri A, Eisenberg DS, et al. Amyloid nomenclature 2022: Update, novel proteins, and recommendations by the International Society of Amyloidosis (ISA) Nomenclature Committee. Amyloid. 2022;29:213–9.
2. Falk RH, Alexander KM, Liao R, Dorbala S. AL (light-chain) cardiac amyloidosis: A review of diagnosis and therapy. J Am Coll Cardiol. 2016;68:1323–41.
3. Ruberg FL, Grogan M, Hanna M, Kelly JW, Maurer MS. Transthyretin Amyloid Cardiomyopathy: JACC State-of-the-Art Review. J Am Coll Cardiol. 2019;73:2872–91.
4. Merlini G, Bellotti V. Molecular mechanisms of amyloidosis. N Engl J Med. 2003;349:583–96.
5. Dorbala S, Cuddy S, Falk RH. How to image cardiac amyloidosis: A practical approach. JACC Cardiovasc Imaging. 2020;13:1368–83.
6. Falk RH. Diagnosis and management of the cardiac amyloidoses. Circulation. 2005;112:2047–60.
7. Bulawa CE, Connelly S, DeVit M, et al. Tafamidis, a potent and selective transthyretin kinetic stabilizer that inhibits the amyloid cascade. Proc Natl Acad Sci. 2012;109:9629–34.
8. Sanguinetti C, Minniti M, Susini V, et al. The journey of human transthyretin: synthesis, structure stability, and catabolism. Biomedicines. 2022;10:1906.
9. Dorbala S, Ando Y, Bokhari S, et al. ASNC/AHA/ASE/EANM/HFSA/ISA/SCMR/SNMMI expert consensus recommendations for multimodality imaging in cardiac amyloidosis: part 1 of 2-evidence base and standardized methods of imaging. J Nucl Cardiol. 2019;26:2065–123.
10. Dorbala S, Ando Y, Bokhari S, et al. ASNC/AHA/ASE/EANM/HFSA/ISA/SCMR/SNMMI expert consensus recommendations for multimodality imaging in cardiac amyloidosis: part 2 of 2-diagnostic criteria and appropriate utilization. J Nucl Cardiol. 2020;27:659–73.
11. Dorbala S, Kijewski MF. Molecular imaging of systemic and cardiac amyloidosis: Recent advances and focus on the future. J Nucl Med. 2023;64:20S-28S.
12. Guy CD, Jones CK. Abdominal fat pad aspiration biopsy for tissue confirmation of systemic amyloidosis: Specificity, positive predictive value, and diagnostic pitfalls. Diagn Cytopathol. 2001;24:181–5.
13. Dasari S, Theis JD, Vrana JA, et al. Amyloid typing by mass spectrometry in clinical practice: A comprehensive review of 16,175 samples. Mayo Clin Proc. 2020;95:1852–64.
14. Linke RP. On typing amyloidosis using immunohistochemistry. Detailled illustrations, review and a note on mass spectrometry. Prog Histochem Cytochem. 2012;47:61–132.
15. Maceira AM, Joshi J, Prasad SK, et al. Cardiovascular magnetic resonance in cardiac amyloidosis. Circulation. 2005;111:186–93.
16. Mongeon FP, Jerosch-Herold M, Coelho-Filho OR, Blankstein R, Falk RH, Kwong RY. Quantification of extracellular matrix expansion by CMR in infiltrative heart disease. JACC Cardiovasc Imaging. 2012;5:897–907.
17. Gillmore JD, Maurer MS, Falk RH, et al. Nonbiopsy diagnosis of cardiac transthyretin amyloidosis. Circulation. 2016;133:2404–12.
18. Dorbala S, Park MA, Cuddy S, et al. Absolute quantitation of cardiac (99m)Tc-pyrophosphate using cadmium-zinc-telluride-based SPECT/CT. J Nucl Med. 2021;62:716–22.
19. Clerc OF, Cuddy SAM, Robertson M, et al. Cardiac amyloid quantification using (124)I-evuzamitide ((124)I-P5+14) versus (18)F-florbetapir: A pilot PET/CT study. JACC Cardiovasc Imaging. 2023;16:1419–32.
20. Khor YM, Cuddy SAM, Singh V, Falk RH, Di Carli MF, Dorbala S. (99m)Tc bone-avid tracer cardiac scintigraphy: Role in noninvasive diagnosis of transthyretin cardiac amyloidosis. Radiology. 2023;306:e221082.
21. Singh V, Falk R, Di Carli MF, Kijewski M, Rapezzi C, Dorbala S. State-of-the-art radionuclide imaging in cardiac transthyretin amyloidosis. J Nucl Cardiol. 2019;26:158–73.
22. Dilsizian V, Bacharach SL, Beanlands RS, et al. ASNC imaging guidelines/SNMMI procedure standard for positron emission tomography (PET) nuclear cardiology procedures. J Nucl Cardiol. 2016;23:1187–226.
23. Kim YJ, Ha S, Kim YI. Cardiac amyloidosis imaging with amyloid positron emission tomography: A systematic review and meta-analysis. J Nucl Cardiol. 2020;27:123–32.
24. Wu Z, Yu C. Diagnostic performance of CMR, SPECT, and PET imaging for the detection of cardiac amyloidosis: A meta-analysis. BMC Cardiovasc Disord. 2021;21:482.
25. Uzuegbunam BC, Librizzi D, Hooshyar Yousefi B. PET radiopharmaceuticals for Alzheimer's disease and Parkinson's disease diagnosis, the current and future landscape. Molecules. 2020;25:977.
26. Martin EB, Williams A, Heidel E, Macy S, Kennel SJ, Wall JS. Peptide p5 binds both heparinase-sensitive glycosaminoglycans and fibrils in patient-derived AL amyloid extracts. Biochem Biophys Res Commun. 2013;436:85–9.
27. Wall JS, Martin EB, Richey T, et al. Preclinical validation of the heparin-reactive peptide p5+14 as a molecular imaging agent for visceral amyloidosis. Molecules. 2015;20:7657–82.
28. Abulizi M, Sifaoui I, Wuliya-Gariepy M, et al. (18)F-sodium fluoride PET/MRI myocardial imaging in patients with suspected cardiac amyloidosis. J Nucl Cardiol. 2021;28:1586–95.
29. Andrews JPM, Trivieri MG, Everett R, et al. 18F-fluoride PET/MR in cardiac amyloid: A comparison study with aortic stenosis and age- and sex-matched controls. J Nucl Cardiol. 2022;29:741–9.
30. Morgenstern R, Yeh R, Castano A, Maurer MS, Bokhari S. (18)Fluorine sodium fluoride positron emission tomography, a potential biomarker of transthyretin cardiac amyloidosis. J Nucl Cardiol. 2018;25:1559–67.
31. Trivieri MG, Dweck MR, Abgral R, et al. (18)F-sodium fluoride PET/MR for the assessment of cardiac amyloidosis. J Am Coll Cardiol. 2016;68:2712–4.
32. Antoni G, Lubberink M, Estrada S, et al. In vivo visualization of amyloid deposits in the heart with 11C-PIB and PET. J Nucl Med. 2013;54:213–20.
33. Lee SP, Lee ES, Choi H, et al. (11)C-Pittsburgh B PET imaging in cardiac amyloidosis. JACC Cardiovasc Imaging. 2015;8:50–9.

34. Pilebro B, Arvidsson S, Lindqvist P, et al. Positron emission tomography (PET) utilizing Pittsburgh compound B (PIB) for detection of amyloid heart deposits in hereditary transthyretin amyloidosis (ATTR). J Nucl Cardiol. 2018;25:240–8.
35. Takasone K, Katoh N, Takahashi Y, et al. Non-invasive detection and differentiation of cardiac amyloidosis using (99m)Tc-pyrophosphate scintigraphy and (11)C-Pittsburgh compound B PET imaging. Amyloid. 2020;27:266–74.
36. Rosengren S, Skibsted Clemmensen T, Tolbod L, et al. Diagnostic accuracy of [(11)C]PIB positron emission tomography for detection of cardiac amyloidosis. JACC Cardiovasc Imaging. 2020;13:1337–47.
37. Choi YJ, Koh Y, Lee HJ, et al. Independent prognostic utility of (11)C-Pittsburgh compound B PET in patients with light-chain cardiac amyloidosis. J Nucl Med. 2022;63:1064–9.
38. Park MA, Padera RF, Belanger A, et al. 18F-florbetapir binds specifically to myocardial light chain and transthyretin amyloid deposits: autoradiography study. Circ Cardiovasc Imaging. 2015;8:e002954.
39. Dorbala S, Vangala D, Semer J, et al. Imaging cardiac amyloidosis: A pilot study using (18)F-florbetapir positron emission tomography. Eur J Nucl Med Mol Imaging. 2014;41:1652–62.
40. Ehman EC, El-Sady MS, Kijewski MF, et al. Early detection of multiorgan light-chain amyloidosis by whole-body (18)F-florbetapir PET/CT. J Nucl Med. 2019;60:1234–9.
41. Gertz MA, Comenzo R, Falk RH, et al. Definition of organ involvement and treatment response in immunoglobulin light chain amyloidosis (AL): A consensus opinion from the 10th International Symposium on Amyloid and Amyloidosis. Am J Hematol. 2005;79:319–28.
42. Baratto L, Park SY, Hatami N, et al. (18)F-florbetaben whole-body PET/MRI for evaluation of systemic amyloid deposition. EJNMMI Res. 2018;8:66.
43. Ezawa N, Katoh N, Oguchi K, Yoshinaga T, Yazaki M, Sekijima Y. Visualization of multiple organ amyloid involvement in systemic amyloidosis using (11)C-PiB PET imaging. Eur J Nucl Med Mol Imaging. 2018;45:452–61.
44. Mestre-Torres J, Lorenzo-Bosquet C, Cuberas-Borros G, et al. Utility of the (18)F-florbetapir positron emission tomography in systemic amyloidosis. Amyloid. 2018;25:109–14.
45. Wagner T, Page J, Burniston M, et al. Extracardiac (18)F-florbetapir imaging in patients with systemic amyloidosis: More than hearts and minds. Eur J Nucl Med Mol Imaging. 2018;45:1129–38.
46. Khor YM, Cuddy S, Harms HJ, et al. Quantitative [(18)F]florbetapir PET/CT may identify lung involvement in patients with systemic AL amyloidosis. Eur J Nucl Med Mol Imaging. 2020;47:1998–2009.
47. Khoor A, Colby TV. Amyloidosis of the lung. Arch Pathol Lab Med. 2017;141:247–54.
48. Cuddy SAM, Bravo PE, Falk RH, et al. Improved quantification of cardiac amyloid burden in systemic light chain amyloidosis: Redefining early disease? JACC Cardiovasc Imaging. 2020;13:1325–36.
49. Datar Y, Clerc OF, Cuddy SAM, et al. Quantification of right ventricular amyloid burden with 18F-florbetapir positron emission tomography/computed tomography and its association with right ventricular dysfunction and outcomes in light-chain amyloidosis. Eur Heart J Cardiovasc Imaging. 2024;25:687–97.
50. Slivnick J, Zareba KM, Varghese J, et al. Prevalence and haemodynamic profiles of pulmonary hypertension in cardiac amyloidosis. Open Heart. 2022;9:e001808.
51. Clerc OF, Datar Y, Cuddy SAM, et al. Prognostic value of left ventricular 18F-florbetapir uptake in systemic light-chain amyloidosis. JACC Cardiovasc Imaging. 2024;17:911–22.
52. Law WP, Wang WY, Moore PT, Mollee PN, Ng AC. Cardiac amyloid imaging with 18F-Florbetaben PET: A pilot study. J Nucl Med. 2016;57:1733–9.
53. Kircher M, Ihne S, Brumberg J, et al. Detection of cardiac amyloidosis with (18)F-Florbetaben-PET/CT in comparison to echocardiography, cardiac MRI and DPD-scintigraphy. Eur J Nucl Med Mol Imaging. 2019;46:1407–16.
54. Dietemann S, Nkoulou R. Amyloid PET imaging in cardiac amyloidosis: A pilot study using (18)F-flutemetamol positron emission tomography. Ann Nucl Med. 2019;33:624–8.
55. Papathanasiou M, Kessler L, Carpinteiro A, et al. (18)F-flutemetamol positron emission tomography in cardiac amyloidosis. J Nucl Cardiol. 2022;29:779–89.
56. Wall JS, Martin EB, Endsley A, et al. First in human evaluation and dosimetry calculations for peptide (124)I-p5+14-a novel radiotracer for the detection of systemic amyloidosis using PET/CT imaging. Mol Imaging Biol. 2022;24:479–88.
57. Foster JS, Balachandran M, Hancock TJ, et al. Development and characterization of a prototypic pan-amyloid clearing agent - a novel murine peptide-immunoglobulin fusion. Front Immunol. 2023;14:1275372.
58. Wall JS, Martin EB, Lands R, et al. Cardiac Amyloid Detection by PET/CT Imaging of Iodine ((124)I) Evuzamitide ((124)I-p5+14): A Phase 1/2 Study. JACC Cardiovasc Imaging. 2023;16:1433–48.
59. Uzuegbunam BC, Librizzi D, Yousefi BH. PET radiopharmaceuticals for Alzheimer's disease and Parkinson's disease diagnosis, the current and future landscape. Molecules. 2020;25:977.